

Masaru Shibata¹, Stuart L. Shapiro^{2,3}, and Kōji Uryū⁴¹*Graduate School of Arts and Sciences, University of Tokyo,
Komaba, Meguro, Tokyo 153-8902, Japan*²*Department of Physics, University of Illinois at Urbana-Champaign, Urbana, IL 61801, USA*³*Department of Astronomy and NCSA, University of Illinois at Urbana-Champaign, Urbana, IL 61801, USA*⁴*Department of Physics, University of Wisconsin at Milwaukee, Milwaukee, WI 53201, USA*

We investigate the equilibrium and stability of supermassive stars of mass $M \gtrsim 10^5 M_\odot$ in binary systems. We find that corotating binaries are secularly unstable for close, circular orbits with $r \lesssim 4R(M/10^6 M_\odot)^{1/6}$ where r is the orbital separation and R the stellar radius. We also show that corotation cannot be achieved for distant orbits with $r \gtrsim 12R(M/10^6 M_\odot)^{-11/24}$, since the timescale for viscous angular momentum transfer associated with tidal torques is longer than the evolution timescale due to emission of thermal radiation. These facts suggest that the allowed mass range and orbital separation for corotating supermassive binary stars is severely restricted. In particular, for supermassive binary stars of large mass $M \gtrsim 6 \times 10^6 M_\odot$, corotation cannot be achieved, as viscosity is not adequate to mediate the transfer between orbital and spin angular momentum. One possible outcome for binary supermassive stars is the onset of quasi-radial, relativistic instability which drives each star to collapse prior to merger: We discuss alternative outcomes of collapse and possible spin states of the resulting black holes. We estimate the frequency and amplitude of gravitational waves emitted during several inspiral and collapse scenarios.

I. INTRODUCTION

Recent astronomical observations provide increasingly strong evidence that supermassive black holes of mass $\sim 10^6 - 10^{10} M_\odot$, exist and that they are the central engines of active galactic nuclei and quasars [1]. In addition to their importance for a fundamental understanding of active galactic nuclei and quasars, gravitational waves from the formation of the supermassive black holes and from inspiraling supermassive binary black holes are likely sources for proposed laser interferometric gravitational wave detectors in space, such as the Laser Interferometer Space Antenna (LISA) [2,3]. However, the scenario by which supermassive black holes form is still uncertain. Viable stellar dynamical and hydrodynamical routes leading to the formation of supermassive black holes have been proposed (see, e.g., [4]). In one hydrodynamical scenario, a supermassive gas cloud is build up from the multiple collisions of stars or small gas clouds in stellar clusters to form a supermassive star. Supermassive stars subsequently collapse to black holes after quasi-stationary contraction as a result of cooling [5,6]. Such a scenario for forming a supermassive star and black hole has been investigated in detail in the 1960s and 70s using simple analytical models or assuming spherical symmetry (see, e.g., [7] for a review and references).

Supermassive stars are likely to be rapidly rotating (see, e.g., [8]). For studies of rapidly rotating stars in equilibrium, it is necessary to perform numerical computations using modern numerical techniques [9] which were not feasible until quite recently. Baumgarte and Shapiro recently performed a detailed numerical analysis of a rapidly rotating supermassive star [7]. Because of the fact that the viscous or magnetic braking timescale for angular momentum transfer is likely to be shorter than the evolution timescale of supermassive stars in the typical mass range, the star can be assumed to be in rigid rotation at the mass-shedding limit (which implies that the spin angular velocity of each star is equal to the Kepler velocity) [10]. They find that at the onset of quasi-radial collapse, the non-dimensional spin parameter cS/GM^2 , where S, M, c and G are spin, mass, light velocity, and gravitational constant, is nearly equal to unity, so that rotating supermassive stars might not collapse directly to a black hole. They speculate that the collapse may be inhibited, forming a disk and/or a bar, or possibly fragmenting into several blobs. If such non-axisymmetric structures form during the collapse, quasi-periodic gravitational waves of $\sim 10^{-4} - 10^{-2}$ Hz may be emitted and provide a strong source for laser interferometric gravitational wave detectors in space [2].

In this paper, we consider supermassive stars in binary systems. Such binaries may arise naturally from fragmentation of a large gas cloud with rapid rotation, or during multiple mergers of small gas clouds and/or stars [4,8]. Even in binary systems, each supermassive star is likely to reach quasi-radial instability eventually after quasi-stationary contraction. In binaries, most of the angular momentum of the system can be distributed in orbital motion so that

the spin of each star may be much smaller than that for isolated supermassive stars. In particular, small spin can be achieved for the case when viscous transport between orbital and spin angular momentum is effective. If so, each star is in slow rotation with respect to the inertial frame, and collapse to a black hole may proceed in an almost spherical manner, with tiny emission of gravitational waves. Thus, the scenario for forming black holes in binary systems could be considerably different from that for isolated supermassive stars. Also, a binary containing supermassive stars can be a progenitor of an inspiraling, supermassive black hole binary in a close orbit. Such a binary can emit gravitational waves in the frequency range appropriate for LISA [see Eq. (6.1)]. To detect gravitational waves from binaries using matched filtering technique [11,12], it is useful to anticipate possible mass and spin states of the black holes. With this motivation, we investigate the equilibrium and stability of supermassive binary stars in this paper.

The paper is organized as follows. In Sec. II, we estimate various timescales which are relevant for evolution of supermassive binary stars. In Sec. III, we construct analytical equilibrium models of corotating, supermassive binary stars and investigate their stability. In Sec. IV, we present numerical solutions for corotating, supermassive binary stars to demonstrate that the analytical results shown in Sec. III are qualitatively correct. In Sec. V, we consider the evolution of corotating, supermassive binary stars as a result of thermal radiation, and clarify their final fate. In Sec. VI, we briefly discuss gravitational waves from supermassive stars in the present scenarios. Section VII is devoted to a brief summary. Hereafter, we adopt the geometrical unit in which $G = c = 1$.

II. TIMESCALES

In this paper, we investigate equilibrium and stability of supermassive stars in close binary systems. Before proceeding, we estimate the relevant timescales characterizing such systems to clarify possible states of supermassive binaries. Here, we define supermassive stars to be self-gravitating objects of mass larger than $\sim 10^5 M_\odot$ (see discussion below). Also, we assume that the binary is an isolated system; namely, the accretion of mass and heating from outside are assumed to be negligible.

The equation of state for supermassive stars is dominated by thermal radiation pressure with a small correction due to baryonic gas pressure. Such stars are convective with constant entropy per baryon [5,6,8]. These conditions imply that the structure of the supermassive stars is very close to that of an $n = 3$ polytrope so that

$$P = K\rho^{4/3} + P_g, \quad P_g \ll K\rho^{4/3}, \quad (2.1)$$

where P , ρ , P_g , and K are the total pressure, baryon mass density, gas pressure, and polytropic constant, respectively; K is approximately related to the entropy of radiation, s_r , according to [5,6]

$$K = \frac{a}{3} \left(\frac{3s_r}{4m_H a} \right)^{4/3}. \quad (2.2)$$

Here, a is the radiation density constant, and m_H the mass of hydrogen; we assume that supermassive stars are composed of pure hydrogen for simplicity. For $n = 3$ spherical polytropes in Newtonian theory, the mass M is uniquely determined by K according to

$$M = \left(\frac{k_1 K}{k_2} \right)^{3/2}, \quad (2.3)$$

where k_1 and k_2 are constants of order unity associated with the Lane-Emden function (see Sec. III). Using this relation, s_r can be written approximately as [6]

$$\frac{s_r}{k} \simeq 0.942 \left(\frac{M}{M_\odot} \right)^{1/2}, \quad (2.4)$$

where k denotes the Boltzmann constant.

In Newtonian theory, pure $n = 3$ spherical polytropes are marginally stable to radial collapse, and with a tiny general relativistic (GR) correction, they are unconditionally unstable. To stabilize such a star, some additional perturbations are necessary. One perturbation is spin angular momentum. As shown in [7], supermassive stars are stabilized if they have a large spin angular velocity. However, in this paper, we mainly analyze corotating, supermassive binary stars, whereby the spin angular momentum of each star is not large enough to stabilize the star against radial collapse. To stabilize such slowly rotating supermassive stars, the role of baryonic gas pressure, which constitutes a small fraction of the total pressure, is crucial.

The evolution of isolated supermassive stars that do not have large angular momentum and are stabilized by the gas pressure has been investigated in detail many years ago [5,6]. According to a typical scenario, a supermassive star shrinks quasi-statically as a result of emission of the thermal radiation from its surface until it reaches a critical point where a GR instability sets in against radial collapse. The radial instability occurs for a critical compactness [13] [see also Eq. (3.24)]

$$\frac{M}{R} > 0.445 \left(\Gamma - \frac{4}{3} \right), \quad (2.5)$$

where R is the circumferential radius, and Γ is the effective adiabatic constant. Here, Γ may be approximately written as

$$\Gamma \simeq \frac{4}{3} + \frac{\beta}{6}, \quad (2.6)$$

where β is the ratio of the gas pressure to the radiation pressure, $\beta \equiv P_g/(K\rho^{4/3}) \ll 1$, which can be expressed as [6]

$$\beta = \frac{8k}{s_r} \simeq 8.5 \left(\frac{M}{M_\odot} \right)^{-1/2}. \quad (2.7)$$

Thus, the constraint of M/R for a stable supermassive star of mass M can be rewritten as

$$\frac{M}{R} \lesssim 0.63 \left(\frac{M}{M_\odot} \right)^{-1/2}. \quad (2.8)$$

In this evolutionary scenario, there are two relevant timescales; the emission timescale of thermal radiation and the dynamical timescale. Supermassive stars emit the thermal radiation from the stellar surface with the Eddington luminosity

$$L_{\text{Edd}} = \frac{4\pi M}{\kappa_T}, \quad (2.9)$$

where κ_T is the opacity with respect to the Thomson scattering. The total energy of a supermassive star is approximately [5,6]

$$E \simeq -\beta \frac{M^2}{R}. \quad (2.10)$$

Thus, the emission timescale of thermal radiation is

$$\tau_{\text{evol}} \equiv \frac{|E|}{L_{\text{Edd}}} \sim 1.4 \times 10^{10} \text{sec} \left(\frac{M/R}{10^{-3}} \right) \left(\frac{\beta}{10^{-3}} \right), \quad (2.11)$$

where, in evaluating κ_T , we assume pure ionized hydrogen. The dynamical timescale is approximately

$$\tau_{\text{dyn}} \equiv \rho_c^{-1/2} \simeq 1.4 \times 10^4 \text{sec} \left(\frac{M/R}{10^{-3}} \right)^{-3/2} \left(\frac{M}{10^6 M_\odot} \right), \quad (2.12)$$

where ρ_c denotes the maximum (central) density of supermassive stars which, for $n = 3$ spherical polytropes, can be expressed as $\rho_c \simeq 12.94 M/R^3$ (see next section and Table I).

For a star to evolve quasi-statically, the inequality, $\tau_{\text{evol}} > \tau_{\text{dyn}}$, must be satisfied, so that

$$\frac{M}{R} > 1.7 \times 10^{-6} \left(\frac{M}{10^6 M_\odot} \right)^{3/5}, \quad (2.13)$$

where we use Eq. (2.7) for evaluating β . From the requirement of stability, M/R also has to satisfy Eq. (2.8). Thus, for existence of a stable supermassive star in quasi-static evolution, the mass has to be less than $\sim 2 \times 10^8 M_\odot$. If the mass is larger than this value, supermassive stars collapse dynamically without evolving through a quasi-static phase. Furthermore, supermassive stars of mass $M \lesssim 10^5 M_\odot$ reach sufficiently high temperature for nuclear burning to become important before reaching the onset of the instability. If nuclear reactions set in, the temperature increases

so rapidly that the star undergoes a violent explosion [14]. Thus, we restrict our attention to stars with $M \gtrsim 10^5 M_\odot$ which are stable until they reach the onset of radial instability.

For binary systems, several additional timescales have to be taken into account. One is the radiation-reaction timescale of gravitational waves, which is written using the quadrupole formula as [15]

$$\tau_{\text{GW}} \simeq \frac{5}{512} \frac{r^4}{M^3} \simeq 2 \times 10^{14} \text{sec} \left(\frac{r/M}{10^3} \right)^4 \left(\frac{M}{10^6 M_\odot} \right), \quad (2.14)$$

where we assume that the mass of each star, M , is identical (i.e., the total mass is $2M$), and where r denotes the orbital separation between two centers of mass. Since $r/M > R/M \gtrsim 10^3$ for stable supermassive stars with $M \geq 10^5 M_\odot$, we immediately find $\tau_{\text{GW}} \gg \tau_{\text{dyn}}$ and $\tau_{\text{GW}} \gg \tau_{\text{evol}}$, so that gravitational radiation reaction is not relevant in this problem.

According to standard scenarios, supermassive stars were formed near galaxy centers in the early stage of galaxy formation [4]. Associated with galaxy formation in its early stage, gas may settle toward the center of the galaxies. If the gas accretes onto supermassive binary stars, it can be a source of friction which can decelerate the orbital motion of the stars. The dragging timescale can be written crudely as

$$\tau_{\text{drag}} \sim \frac{M}{\rho_0 R^2 r \Omega} \sim \frac{4\pi}{3} \left(\frac{\rho_c}{\rho_m} \right)^{1/2} \left(\frac{\rho_m}{\rho_0} \right) \left(\frac{r}{R} \right)^{1/2} \tau_{\text{dyn}}, \quad (2.15)$$

where ρ_0 and ρ_m denote the typical density of the accreting gas, and the mean density of supermassive stars. If $\tau_{\text{drag}} < \tau_{\text{evol}}$ the orbital decay due to friction can become effective in inducing merging. However, to achieve this condition, ρ_0 has to be extraordinary large,

$$\rho_0 \gtrsim 10^{-9} \text{g/cm}^3 \left(\frac{M/R}{10^{-3}} \right)^{1/2} \left(\frac{M}{10^6 M_\odot} \right)^{-1/2} \left(\frac{r}{2R} \right)^{1/2}, \quad (2.16)$$

implying that ρ_0 has to be larger than $\sim 10^{13} M_\odot/\text{pc}^3$. Also, the total amount of mass of the accreted gas in time τ_{evol} has to be as large as $\sim M$ so that the binary in such situation cannot be regarded as an isolated system contrary to our assumption in Sec. II. Thus, we do not consider the effect of the friction.

The viscous timescale plays an important role in determining the velocity field in binary systems. Here, we have to take into account two timescales. One is associated with the tidal torque from the companion star (hereafter, we refer to this viscous timescale as τ_{vis}). If τ_{vis} is shorter than τ_{evol} , transfer between orbital and spin angular momentum can be efficient and corotation is achieved. On the other hand, for $\tau_{\text{vis}} > \tau_{\text{evol}}$, angular momentum transfer is not important, implying that the spin of each star is determined solely by the viscous angular momentum transfer inside each star (hereafter, we refer to this timescale as τ_{vis0}). In the case when $\tau_{\text{vis}} > \tau_{\text{evol}} > \tau_{\text{vis0}}$, each star will be in rigid rotation in its comoving frame. For $\tau_{\text{vis}} > \tau_{\text{vis0}} > \tau_{\text{evol}}$, vorticity of stars is conserved, but such a high value of τ_{vis0} is unlikely [see below Eq. (2.24)].

The timescale for the viscous transfer of the angular momentum induced by the tidal torque is approximately [16]

$$\tau_{\text{vis}} \sim \frac{R^2}{\nu} \left(\frac{r}{R} \right)^6, \quad (2.17)$$

where ν is the viscous parameter. As often found in astrophysical contexts, microscopic, molecular viscosity yields timescales that are larger than the evolutionary timescale by many orders of magnitude. However, the effect of turbulent viscosity can be estimated by assuming that the velocity of turbulent motion v_t is an appreciable fraction of the velocity of sound [17],

$$v_t = \alpha v_{\text{sound}}, \quad (2.18)$$

where we take the dimensionless viscosity parameter α to be in the range $0.01 \lesssim \alpha \lesssim 1$. Assuming the characteristic length scale of turbulence to be of $O(R)$, we can estimate ν as

$$\nu \sim \alpha R v_{\text{sound}}. \quad (2.19)$$

Then,

$$\tau_{\text{vis}} \sim \frac{R}{\alpha v_{\text{sound}}} \left(\frac{r}{R} \right)^6 \sim \alpha^{-1} \left(\frac{r}{R} \right)^6 \tau_{\text{dyn}}. \quad (2.20)$$

To achieve corotation, the condition $\tau_{\text{vis}} < \tau_{\text{evol}}$ has to apply, and hence,

$$\frac{r}{R} \lesssim 14\alpha^{1/6} \left(\frac{M/R}{10^{-3}} \right)^{5/12} \left(\frac{M}{10^6 M_\odot} \right)^{-1/4}. \quad (2.21)$$

Since M/R has to satisfy Eq. (2.8), we obtain

$$\frac{r}{R} \lesssim 12\alpha^{1/6} \left(\frac{M}{10^6 M_\odot} \right)^{-11/24}. \quad (2.22)$$

The existence of binary systems requires r to be larger than $\sim 2R$, implying

$$M < 5 \times 10^7 \alpha^{4/11} M_\odot. \quad (2.23)$$

Therefore, supermassive stars in corotating binaries can exist only for close orbits [cf. Eq. (2.21)], for compact stars [cf. Eq. (2.22)], and for a fairly small mass [cf. Eq.(2.23)]. In particular, supermassive stars in binary systems with masses larger than $\sim 10^8 M_\odot$ cannot be in corotation. In the next section, we will show that the stability may further restrict the allowed region for these parameters.

Even if tidal interactions are not important, the viscous transfer of angular momentum inside each star can be important [7], since the viscous timescale is

$$\tau_{\text{vis0}} \sim \alpha^{-1} \tau_{\text{dyn}}. \quad (2.24)$$

Thus, as long as $M/R > 1.7 \times 10^{-6} \alpha^{-2/5} (M/10^6 M_\odot)^{3/5}$, the relation $\tau_{\text{vis0}} < \tau_{\text{evol}}$ always holds.

III. ANALYTICAL MODEL FOR COROTATING BINARY

We investigate the stability of supermassive binary stars supported by a polytropic equation of state

$$P = K\rho^\Gamma. \quad (3.1)$$

In this section, Γ is chosen to be close to $4/3$ according to

$$\Gamma = \frac{4}{3} + \epsilon, \quad \epsilon = \frac{\beta}{6} \ll 1. \quad (3.2)$$

With this choice of equation of state, we can investigate the quantitative properties of supermassive stars of mass $M \gg M_\odot$ analytically by means of a variational principle. As mentioned in Sec. II, such stars have an effective adiabatic constant given approximately by

$$\Gamma \simeq \frac{4}{3} + 1.42 \left(\frac{M}{M_\odot} \right)^{-1/2}. \quad (3.3)$$

If we assume that the mass of supermassive stars is in the range between $10^5 M_\odot$ and $2 \times 10^8 M_\odot$, ϵ should be in the range between $\sim 10^{-4}$ and $\sim 5 \times 10^{-3}$ [Eq. (2.7)].

We here consider corotating supermassive stars of equal mass for simplicity. The alternative extreme case of binary component with large mass ratios is also investigated in Appendix A using a Roche binary model. There we show that the results are qualitatively the same. To determine equilibrium and stability of supermassive stars in corotating binary systems, we write the total energy for each star as the sum of the internal energy U , the potential energy W , the orbital kinetic energy T , the spin kinetic energy T_s and the binding energy between two stars W_b as [6,18]

$$U = k_1 K M x^{n/3}, \quad (3.4)$$

$$W = -k_2 M^{5/3} x - k_4 M^{7/3} x^2, \quad (3.5)$$

$$T = \frac{M}{8} r^2 \Omega^2, \quad (3.6)$$

$$T_s = \frac{1}{2} I \Omega^2, \quad (3.7)$$

$$W_b = -\frac{M^2}{2r}. \quad (3.8)$$

Here, M is the mass of each star, $x = \rho_c^{1/3}$ the density parameter (ρ_c is the maximum density again), r the orbital separation between the two centers of mass, $n [= 1/(\Gamma - 1)]$ the polytropic index, Ω the orbital angular velocity, and I the moment of inertia. We do not distinguish the rest mass (baryon mass) and gravitational mass since their difference is quite small and unimportant for supermassive stars. The nondimensional structure constants k_1 , k_2 , and k_4 are constants dependent on n calculated from the Lane-Emden function [6]. In Table I, we list these constants for several n near 3.

In W , we include the first post-Newtonian correction taking into account GR effects on the stability against quasi-radial collapse. We neglect the first post-Newtonian corrections in W_b since their magnitude is smaller than that of the Newtonian terms by several orders of magnitude as $M/r < M/2R \ll 1$. We also neglect the tidal energy in W_b and W [19]. As we estimate the magnitude of this effect in Appendix B, it is not substantial for corotating binaries. As long as $\epsilon \gtrsim 7 \times 10^{-4}$, it is not important even in non-spinning binaries.

The quantity I may be written in the form

$$I = \kappa M^{5/3} \rho_c^{-2/3}, \quad (3.9)$$

where κ is a constant calculated from the Lane-Emden function (cf. Table I).

The total energy per one star, E , then becomes

$$E = k_1 K M x^{3/n} - k_2 M^{5/3} x - k_4 M^{7/3} x^2 + \left(\frac{Mr^2}{8} + \frac{I}{2} \right) \Omega^2 - \frac{M^2}{2r}. \quad (3.10)$$

The equilibrium angular velocity Ω is derived from the relation $\partial E / \partial r|_{M,J,K} = 0$ as

$$\Omega = \sqrt{\frac{2M}{r^3}}, \quad (3.11)$$

where J is the angular momentum of one star

$$J = \frac{Mr^2\Omega}{4} + I\Omega = (\eta\Omega^{-1/3} + \kappa x^{-2}\Omega)M^{5/3}, \quad (3.12)$$

and $\eta = 2^{-4/3}$. We note that the second term denotes the spin of each star $S(= I\Omega)$.

Substituting $r = (2M/\Omega^2)^{1/3}$ in E and taking the first derivative of $E(= E[x, \Omega(x)])$ with respect to x , fixing M , J and K , yields a second condition for equilibrium,

$$0 = \frac{\partial E}{\partial x} \Big|_{M,J,K} = \frac{3k_1}{n} K M x^{3\epsilon} - k_2 M^{5/3} - 2k_4 M^{7/3} x + \frac{\kappa \Omega^2 M^{5/3}}{x^3}, \quad (3.13)$$

where we use $\epsilon = 1/n - 1/3$ and the relation

$$\frac{\partial \Omega}{\partial x} \Big|_{M,J} = \frac{2\kappa}{x^3} \Omega \left(-\frac{\eta}{3} \Omega^{-4/3} + \frac{\kappa}{x^2} \right)^{-1} < 0. \quad (3.14)$$

The second derivative of $E(= E[x, \Omega(x)])$ with respect to x becomes

$$\begin{aligned} \frac{\partial^2 E}{\partial x^2} \Big|_{M,J,K} &= \frac{9\epsilon k_1}{n} K M x^{3\epsilon-1} - 2k_4 M^{7/3} - \frac{3\kappa M^{5/3} \Omega^2}{x^4} \left(\frac{\eta x^2 + \kappa \Omega^{4/3}}{\eta x^2 - 3\kappa \Omega^{4/3}} \right) \\ &= 3\epsilon k_2 M^{5/3} x^{-1} - 2(1 - 3\epsilon) k_4 M^{7/3} - \frac{3\kappa \Omega^2 M^{5/3}}{x^4} \left(\frac{\eta x^2 + \kappa \Omega^{4/3}}{\eta x^2 - 3\kappa \Omega^{4/3}} + \epsilon \right), \end{aligned} \quad (3.15)$$

where to derive the second line, we use Eq. (3.13). For stable equilibrium, this second derivative has to be positive, and the zero point marks the onset of instability [5,6].

It is convenient to analyze equilibrium and stability fixing $\Omega^2/\rho_c = \Omega^2/x^3 \equiv \omega^2$, which is equivalent to fixing the ratio of the orbital separation to the stellar radius of stars:

$$\omega^2 = \frac{8\pi}{3} \left(\frac{R}{r} \right)^3 \left(\frac{\rho_c}{\rho_m} \right)^{-1} \sim 0.02 \left(\frac{2R}{r} \right)^3, \quad (3.16)$$

where ρ_m denotes the mean stellar density, i.e., $3M/(4\pi R^3)$, and $\rho_c/\rho_m \sim 54$ for $\epsilon \ll 1$ (see Table I). Since $r > 2R$ for binary systems, ω^2 should be less than ~ 0.02 . (In reality, ω^2 is less than ~ 0.01 since the equator of each star is significantly enlarged by the centrifugal force associated with the spin for close binaries.)

The equilibrium condition $\partial E/\partial x|_{M,J,K} = 0$ yields the relation between M and x as

$$M = \left[\frac{-(k_2 - \kappa\omega^2) + \sqrt{(k_2 - \kappa\omega^2)^2 + 24k_1k_4Kx^{1+3\epsilon}/n}}{4k_4x} \right]^{3/2}. \quad (3.17)$$

The condition for the onset of instability $\partial^2 E/\partial x^2|_{M,J,K} = 0$ with Eq. (3.17) gives the solution of x at the critical points as

$$x = \left[\frac{3(\epsilon k_2 - \kappa\omega^2 F_0)\{k_2 - \kappa\omega^2(1 + 3F_0 - 3\epsilon)\}}{2(1 - 3\epsilon)^2(1 + 3\epsilon)k_1k_4K} \right]^{n/3} \equiv x_c, \quad (3.18)$$

where

$$F_0 = \frac{\eta + \kappa\omega^{4/3}}{\eta - 3\kappa\omega^{4/3}} + \epsilon. \quad (3.19)$$

Since our purpose here is to determine the stability, we restrict our attention to the case where K is constant. Equation (3.18) implies that on every equilibrium curve, $M(x)$, of a fixed value of ω , there exists one turning point x_c for a sequence along which J is constant as

$$J = (\eta\omega^{-1/3} + \kappa\omega)x_c^{-1/2}M(x_c)^{5/3}. \quad (3.20)$$

However, the implications of the existence of turning points for small ω and large ω are different. Consider the relation between $\bar{M} = MK^{-n/2}$ and $(\bar{\rho}_c)^{(3-n)/2n}$ ($\bar{\rho}_c = \rho_c K^n$) for $\epsilon = 0.003$ in Fig. 1 as an example. We remark that the qualitative behavior is independent of ϵ as long as $0 < \epsilon \lesssim 0.01$. In the presence of a general relativistic effect or in the case $\epsilon > 0$, $MK^{-n/2}$ is not constant even in the infinite separation (i.e., $\omega^2 = 0$), but it is still close to ~ 4.5 for a wide range of the central density and orbital separation as long as $\epsilon \ll 1$. The solid curves denote the relation between \bar{M} and $\bar{\rho}_c$ for $\omega^2 = 0, 0.005$ and 0.01 , and the dotted curve for the sequence of turning points defined by Eqs. (3.17) and (3.18). We also plot the curves of constant \bar{J} where $\bar{J} = JK^{-n}$ (the dashed lines). According to the turning point theorem [20], a change of the sign of $d\bar{M}/d\bar{\rho}_c$ along a curve of constant value of \bar{J} indicates the change of (secular) stability. Along curves of constant \bar{J} , there are in general two turning points for different value of ω at $\bar{\rho}_c = \bar{\rho}_1$ and $\bar{\rho}_2 (> \bar{\rho}_1)$ for $\bar{J} \gtrsim 420$. The turning point at $\bar{\rho}_c = \bar{\rho}_1$ exists only for $\omega \geq \omega_{\text{crit}}$ and that of $\bar{\rho}_2$ for $\omega \leq \omega_{\text{crit}}$. Here, numerical calculation yields the approximate relation

$$\omega_{\text{crit}}^2 \simeq (0.35 - 0.38)\epsilon, \quad \text{for } 10^{-4} \leq \epsilon \leq 5 \times 10^{-3}. \quad (3.21)$$

We can determine the stability for stars along a curve of constant \bar{J} in the following manner. All the curves of constant \bar{J} in Fig. 1 asymptotically approach the unstable branch of isolated spherical stars (the solid curve with $\omega^2 = 0$). Stars on this branch are unstable against radial collapse. This implies that a binary star with $\bar{\rho}_c > \bar{\rho}_2$ is secularly unstable against quasi-radial collapse. Since the stability changes at each turning point, a star with $\bar{\rho}_1 < \bar{\rho}_c < \bar{\rho}_2$ is stable and one with $\bar{\rho}_c < \bar{\rho}_1$ is secularly unstable.

The compactness of star at $x = x_c$ is evaluated as

$$\frac{M}{R} = \frac{3\epsilon k_2}{2(1 - 3\epsilon)k_4} \left(\frac{4\pi\rho_m}{3\rho_c} \right)^{1/3} F \equiv C_c \epsilon F, \quad (3.22)$$

where

$$F \equiv 1 - \frac{\kappa\omega^2}{\epsilon k_2} \left(\frac{\eta + \kappa\omega^{4/3}}{\eta - 3\kappa\omega^{4/3}} + \epsilon \right) \leq 1, \quad (3.23)$$

and where C_c is a constant depending on n (cf. Table I). For $n \rightarrow 3$, we find

$$\frac{M}{R} \simeq 0.445\epsilon F. \quad (3.24)$$

Thus, for $\omega \rightarrow 0$ ($F \rightarrow 1$; infinite separation), we recover the well-known result $M/R = 0.445\epsilon$ for onset of the instability against radial collapse [13]. We note that F is less than unity for finite value of ω . Thus, the compactness

of marginally stable stars against quasi-radial collapse in a corotating binary is smaller than that for spherical stars. This is mainly because the stellar radius is enlarged by the centrifugal force induced by the spin angular momentum S . Figure 1 also shows that the instability to quasi-radial collapse sets in for a slightly smaller central density and a slightly larger mass than those for spherical stars in isolation, for given entropy.

The instability for a star with $\bar{\rho}_c < \bar{\rho}_1$ is not due to the first post-Newtonian effect; namely, it is not associated with quasi-radial collapse. First, we derive the condition for the existence of such an instability. For stable equilibrium, the condition, $\partial^2 E / \partial x^2|_{M,J,K} > 0$, has to be satisfied. Equation (3.15) obviously implies that the following condition is necessary, independent of M and x and irrespective of the first post-Newtonian term:

$$\epsilon k_2 - \kappa \omega^2 \left(\frac{\eta + \kappa \omega^{4/3}}{\eta - 3\kappa \omega^{4/3}} + \epsilon \right) > 0. \quad (3.25)$$

Note that this condition is sufficient to insure stability in the Newtonian case.

Assuming $\omega \ll (\eta/\kappa)^{3/4}$ and $\epsilon \ll 1$, Eq. (3.25) can be approximately written as

$$\omega^2 < \omega_{\min}^2, \quad \omega_{\min}^2 \simeq \frac{\epsilon k_2}{\kappa} \left[\frac{\eta + \kappa(\epsilon k_2/\kappa)^{2/3}}{\eta - 3\kappa(\epsilon k_2/\kappa)^{2/3}} \right]^{-1} \simeq 1.5\epsilon(1 - 2.8\epsilon^{2/3}) \quad (3.26)$$

or

$$r \gtrsim \left(\frac{8\pi\kappa\rho_m}{3k_2\epsilon\rho_c} \right)^{1/3} \left[\frac{\eta + \kappa(\epsilon k_2/\kappa)^{2/3}}{\eta - 3\kappa(\epsilon k_2/\kappa)^{2/3}} \right]^{1/3} R \sim 4.6 \left(\frac{0.001}{\epsilon} \right)^{1/3} (1 + 0.9\epsilon^{2/3}) R, \quad (3.27)$$

where to evaluate k_2 , κ , and ρ_c/ρ_m , we use the value for an $n = 3$ Newtonian spherical polytrope (cf. Table I). Equation (3.26) implies that for a very small value of ϵ (i.e., $\epsilon \lesssim 0.01$) with which $\omega_{\min}^2 \lesssim 0.01$, close orbits with $\omega^2 \gtrsim \omega_{\min}^2$ [see Eq. (3.16)] are secularly unstable; namely, the existence of close corotating binaries may be prohibited when ϵ is too small. It is noteworthy that all corotating binary stars with $\epsilon \rightarrow 0$ are secularly unstable.

In Figs. 2 (a) and (c), we show the relations for \bar{J} and $\bar{\Omega}(=K^{n/2}\Omega)$ as functions of ω^2 for $\epsilon = 0.003$ along a fixed value of \bar{M} (here we choose $\bar{M} = 4.05$ and 3.90). We also show the relation between \bar{J} and $\bar{\Omega}$ near the minimum of \bar{J} in Figs. 2 (b) and (d). As expected from Fig. 1, the curve of \bar{J} has a minimum at $\omega = \omega_{\min}$. For higher mass case $\bar{M} = 4.05$, the GR effect is important so that ω_{\min}^2 is significantly less than the Newtonian value shown in Eq. (3.26), i.e., ~ 0.0042 . However, for $\bar{M} = 3.90$, it approaches this value.

Recall that the turning point theorem specifies nothing about the type of unstable mode or the growth timescale for the secular instability. Thus, we can suggest plausible outcomes. One of the most likely outcomes is that, given some dissipation, a binary with $\omega > \omega_{\min}$ could become secularly unstable to merger as in the case of stiff equation of state with $\Gamma \gtrsim 2$ [18]. [Namely, a corotating supermassive binary appears to have an innermost stable circular orbit (ISCO).] It should be noted that in a binary of supermassive stars, the system evolves as a result of thermal radiation on the time scale τ_{evol} . This implies that the secular instability can play a role only if the secular timescale is as small as τ_{evol} . As discussed in Sec. II, the dissipation timescale due to gravitational waves τ_{GW} is much longer than τ_{evol} . Hence, this secular instability is irrelevant for evolution of supermassive binary stars. However, viscous damping τ_{vis} may be important.

The minimum of \bar{J} (i.e., ISCO) along a sequence of constant \bar{M} appears before two stars come into contact only for restricted values of n (i.e., $n \lesssim 1$ or $|n - 3| \ll 1$). The reason can be explained in the following manner. The angular momentum of one star [cf. Eq.(3.12)] is written in the form

$$J(r) = \frac{M^{3/2}r^{1/2}}{2\sqrt{2}} + \frac{2\sqrt{2}\kappa_n M^{3/2}R^2}{5r^{3/2}}, \quad (3.28)$$

where $\kappa_n = I/(0.4MR^2) = (5\kappa/2)(4\pi\rho_m/3\rho_c)^{2/3}$, which is a monotonically decreasing function of n (for Newtonian polytropes, $\kappa_0 = 1$, $\kappa_1 \simeq 0.653$, and $\kappa_3 \simeq 0.188$ [18]). The ISCO is located by finding zero point of dJ/dr as a function of r , which is calculated as

$$\frac{dJ}{dr} = \frac{M^{3/2}}{2^{5/2}r^{1/2}} \left[1 - \frac{6\kappa_n}{5} \left(\frac{2R}{r} \right)^2 \left(1 - \frac{4r}{3R} \frac{dR}{dr} \right) \right]. \quad (3.29)$$

Here, we note that dR/dr is negative, since the stellar radius is enlarged by the centrifugal force associated with the spin angular momentum which increases with decreasing r . Equation (3.29) implies that the zero point of dJ/dr for corotating binaries is produced by the effect of spin angular momentum and exists for $r \gtrsim 2R$ if κ_n is large enough $\gtrsim 0.8$ or if $|dR/dr|$ is large enough, i.e., of $O(R/r)$, in the case that κ_n is small. For soft equations of state with $n \sim 3$,

κ_n is small ~ 0.188 , but R rapidly increases with decreasing r for close orbits. (Recall that for $n \sim 3$, the equatorial radius increases significantly even with a small magnitude of the spin angular momentum; e.g., for the Kepler spin velocity, the equator increases by a factor of 1.5 for $n = 3$, according to the Roche model [6].) This rapid increase of R with decreasing r produces the ISCO.

As shown in [18,21], ISCOs also exist for sufficiently stiff equations of state with $n \lesssim 1$. In this case, R does not change significantly with decreasing r [18]. However, κ_n is of $O(1)$ for $n \lesssim 1$, resulting in existence of the ISCO. For intermediate range of n with $1 \lesssim n \lesssim 3$, neither the magnitude of κ_n nor the rate of increase of R with decreasing r is sufficient to produce an ISCO.

From Fig. 2, we find that Ω has a maximum at a point where $\omega > \omega_{\min}$. The appearance of this maximum can be explained in the similar manner. Along a corotating binary sequence of fixed values of M and K , ρ_c decreases with increasing ω . However, the orbital frequency $\Omega = \omega \rho_c^{1/2}$ does not have to increase. For sufficiently small ω , the decreasing rate of ρ_c , $d\rho_c/d\omega$, due to increasing spin frequency of each star is so small that Ω increases with ω . For close orbits, on the other hand, the effect of the spin becomes significant enough to enlarge the equator and to decrease ρ_c by a large factor. Then, Ω can decrease with increasing ω .

Assuming that the timescale for secular instability, τ_{vis} , is as short as τ_{evol} , we can constrain the allowed region for existence of supermassive stars in corotating binary systems. For a supermassive star of mass M , ϵ can be written as $1.42(M/M_\odot)^{-1/2}$ [cf. Eq. (3.3)]. Thus, Eq. (3.27) can be rewritten to

$$r > 4.1R \left(\frac{M}{10^6 M_\odot} \right)^{1/6}. \quad (3.30)$$

On the other hand, Eq. (2.22) has to be satisfied for achieving corotation. These two conditions constrain the allowed regions of M and r/R according to

$$4.1 \left(\frac{M}{10^6 M_\odot} \right)^{1/6} \lesssim \frac{r}{R} \lesssim 12\alpha^{1/6} \left(\frac{M}{10^6 M_\odot} \right)^{-11/24}, \quad (3.31)$$

$$M \lesssim 6 \times 10^6 \alpha^{4/15} M_\odot. \quad (3.32)$$

Thus, the existence of supermassive stars in corotating binary systems may be strongly restricted provided the growth timescale of the secular instability is as short as τ_{evol} .

IV. NUMERICAL MODEL FOR COROTATING BINARY

To demonstrate that the analytical model presented in Sec. III is qualitatively correct, we perform numerical computation for equilibrium of corotating, supermassive binary stars. To construct a numerical model, we adopt the conformally flat approximation of general relativity. In this approximation, we solve part of the Einstein field equations assuming that the spatial line element is conformally flat (see, e.g., [21,22] for equations). From the post-Newtonian point of view, this approximation is exact only up to the first post-Newtonian order. However, supermassive stars are not very compact, even at the onset of radial collapse, so that the higher post-Newtonian terms do not play any important role. Thus, the solution derived in this formulation provides an excellent approximation.

To demonstrate that the results in Sec. III are qualitatively correct, we present here only one example setting $\epsilon = 0.003$. The detailed results and detailed analysis for other parameters of the numerical computation will be presented elsewhere.

The computation is performed on a $121 \times 121 \times 121$ Cartesian grid. We here use two numerical codes which were previously implemented to prepare initial conditions for mergers of neutron star binaries [22,23]. Computations were mainly performed in the code by Shibata [22], while the other code [23] was used to confirm the numerical results. The equations are solved in one octant ($x, y, z \geq 0$). We always assign 40 grid points for the major diameter of a supermassive star. Comparing the maximum mass for sufficiently distant orbits with the maximum mass for isolated spherical stars, which can be computed with high accuracy in a one dimensional code, it is found that with this resolution, the mass of the system is systematically underestimated by $\sim 0.8\%$. Hence, our numerical results contain an error of this order. To check the convergence of numerical solutions, we performed computations on a $91 \times 91 \times 91$ grid, covering the major diameter of the star by 30 grid points. In this case, the mass is systematically underestimated by $\sim 1.5\%$, indicating that convergence with increasing the resolution is achieved.

In Fig. 3, we show the dependence of \bar{M}_* versus $\bar{\rho}_c$ (compare with Fig. 1). Here, M_* denotes the rest mass of one star. The solid lines denote the relation between \bar{M}_* and $\bar{\rho}_c$ for fixed values of $\hat{d} \equiv (r_{\text{out}} + r_{\text{in}})/(r_{\text{out}} - r_{\text{in}}) = 1.3, 1.5$, and 3.05 where r_{out} and r_{in} denote the coordinate distance from the origin to the outer and inner edges of star along

the axis which connects the centers of mass of the two stars. $\omega^2 (= \Omega^2/\rho_c)$ is 0.006, 0.0046, and 0.00068 for $\hat{d} = 1.3$, 1.5 and 3.05, respectively. The dashed curves show the relation of \bar{M}_* versus $\bar{\rho}_c$ for constant values of \bar{J} .

As expected from the analytical results for $\bar{J} \gtrsim 410$, the curve for constant \bar{J} has one minimum at $\bar{\rho}_1$ and one maximum at $\bar{\rho}_2 > \bar{\rho}_1$: The former is associated with the ISCO and the latter with the onset of quasi-radial collapse. It is found that the turning point at $\bar{\rho}_1$ approaches to the curve of $\omega^2 \sim 0.0042$ for the Newtonian limit ($\bar{\rho}_1 \rightarrow 0$), as indicated by the analytical study [cf. Eq. (3.26)].

In Fig. 4, we show the relation between \bar{J} and $\bar{\Omega}$ for $\bar{M}_* = 4.04$ near the minimum of \bar{J} [compare with Fig. 2 (b)]. It is seen that the minimum of \bar{J} and the maximum of $\bar{\Omega}$ exist, illustrating that the analytical results presented in Sec. III are qualitatively correct and quantitatively fairly accurate. All these results demonstrate the robustness of analytical modeling for corotating, supermassive binary stars.

V. QUASI-STATIONARY EVOLUTION OF SUPERMASSIVE BINARY STARS

In this section we determine evolutionary sequences of corotating, supermassive binary stars to the onset of instability or merger. As discussed in Sec. II, supermassive stars dissipate energy by thermal radiation. We assume that rest mass is conserved during the evolution, since spin is far below Kepler limit in corotating systems. Although a small amount of mass of system may be ejected due to a stellar wind in reality [5], we neglect such effects for simplicity. Since the timescale of gravitational radiation reaction is too long to dissipate the angular momentum and because of mass conservation, we assume that the angular momentum of the system is also conserved. We also assume that the effective adiabatic constant Γ is unchanged during the evolution for simplicity. Strictly speaking, this assumption is not valid since β depends on the entropy of the radiation which decreases during the evolution. This treatment is adequate only when the fractional decrease in the entropy is not very large.

In this setting, the energy E for an equilibrium star is a function of K and x , i.e., $E(K, x)$, and the evolution equation for E can be written as

$$\dot{E} = k_1 \dot{K} M x^{3/n} + \left. \frac{\partial E}{\partial x} \right|_{M, J, K} \dot{x} = k_1 \dot{K} M x^{3/n}, \quad (5.1)$$

where “ $\dot{}$ ” denotes the time derivative, and where $(\partial E/\partial x)|_{M, J, K} = 0$ since we assume quasi-stationary evolution along an equilibrium track. From this equation, it is immediately found that K decreases with evolution since \dot{E} is negative.

The decrease of K implies that \bar{M} and \bar{J} increase. However, $\bar{J}/\bar{M}^2 = J/M^2$ remains constant. Thus, the evolutionary sequence is specified by the value of \bar{J}/\bar{M}^2 . In Fig. 5, we show \bar{M} as a function of $\bar{\rho}_c$ for a fixed value of $\bar{J}/\bar{M}^2 (= 28, 31 \text{ and } 35)$ and $\epsilon = 0.003$ as an example (thick solid lines). Along these curves, \bar{M} has to increase. This implies that if a corotating binary initially resides in the right-hand side of the dotted curve (which indicates the turning points), $\bar{\rho}_c$ increases with decreasing ω . If a corotating binary resides in the left-hand side of the dotted curve, $\bar{\rho}_c$ decreases with increasing ω . Since we assume that J is conserved, Ω should slightly decrease (increase) with decreasing (increasing) ω in these evolutionary sequences [cf. Eq. (3.14)]. Therefore, if a corotating binary initially resides in the right-hand (left-hand) side of the dotted curve, the orbital separation r slightly increases (decreases) with evolution.

As we found in Sec. III, supermassive stars on the left-hand side of the dotted line are secularly unstable to merger. Thus, if this instability grows in a timescale as short as τ_{evol} , the final fate is not determined by thermal radiation but by the secular dissipation timescale[†]. Only when the system evolves by means of thermal emission, supermassive stars quasi-stationarily evolve with decreasing central density and increasing ω to merger. In either case, the final outcome will likely be a single, rotating supermassive star with a surrounding disk as a result of merger. Such a rotating star will presumably be rapidly rotating, so that its subsequent evolution may be essentially the same as for a single isolated rotating star as discussed in [7].

In the case when the binary resides in the right-hand side of the dotted line, the evolution will proceed via one of several scenarios. If the viscous timescale with regard to the tidal torque is shorter than the thermal evolution timescale throughout the entire evolution, corotation is preserved, and the sequence terminates at the point of unstable, quasi-radial collapse. We refer to this scenario as scenario (A). However, viscosity may not be strong enough to preserve corotating orbits for small ω , i.e., $\omega < \omega_{\text{vis}}$, where [cf. Eqs. (2.21) and (3.16)],

[†]A point of dynamical instability is likely to arise beyond the point of secular instability, but this point cannot be identified by the present treatment that assumes corotation (see, e.g., [18])

$$\omega_{\text{vis}}^2 \sim 5.6 \times 10^{-5} \alpha^{-1/3} \left(\frac{M/R}{10^{-3}} \right)^{-5/4} \left(\frac{M}{10^6 M_\odot} \right)^{3/4} \gtrsim 10^{-4} \alpha^{-1/3} \left(\frac{M}{10^6 M_\odot} \right)^{11/8}. \quad (5.2)$$

Here we use Eq. (2.8) to derive the second inequality. In this case, the orbit may depart from corotation before reaching the turning point. We refer to this scenario as scenario (B).

Scenario (A) is possible only for relatively small mass since the condition $\omega_{\text{crit}} \geq \omega_{\text{vis}}$ is necessary. This condition reduces to

$$\frac{M}{R} \gtrsim 2 \times 10^{-4} \alpha^{-4/15} \left(\frac{M}{10^6 M_\odot} \right), \quad (5.3)$$

$$M \lesssim 4 \times 10^6 \alpha^{4/15} M_\odot. \quad (5.4)$$

Thus, only for supermassive binary stars of fairly small mass and of fairly large compactness, corotation can be preserved until the onset of quasi-radial instability.

Assuming that corotation is preserved through the entire evolution [i.e., scenario (A)], we estimate the non-dimensional, spin parameter of each star, $q \equiv S/M^2$, at the onset of quasi-radial collapse in order to assess the final remnant following the collapse. Since the star in corotation has a spin angular velocity equal to Ω , q is calculated according to

$$q = \frac{I\Omega}{M^2} = \kappa \left(\frac{3\rho_c}{4\pi\rho_m} \right)^{-1/6} \left(\frac{R}{M} \right)^{1/2} \omega. \quad (5.5)$$

Using Eq. (3.22), we find that q at the onset of quasi-radial collapse for $\epsilon \ll 1$ is

$$q = q_0 \omega \epsilon^{-1/2} F^{-1/2}, \quad (5.6)$$

where

$$q_0 \equiv \kappa \left(\frac{2k_4(1-3\epsilon)}{3k_2} \right)^{1/2}; \quad (5.7)$$

values of q_0 are at most ~ 0.4 (cf. Table I). As mentioned in Sec. III, $\omega \leq \omega_{\text{crit}}$ at a turning point for quasi-radial collapse (e.g., the thick dotted line in Fig. 5). With this constraint and Eq. (3.21), Eq. (5.6) reduces to

$$q < 0.6 q_0 F^{-1/2} \sim 0.25 F^{-1/2}. \quad (5.8)$$

Since ω is less than ω_{crit} [cf. Eq. (3.21)] at the onset of quasi-radial collapse, $F \gtrsim 0.5$ [cf. Eq. (3.23)]. Therefore, if quasi-radial instability sets in for supermassive stars in corotating binaries, q has to be much smaller than unity. Consequently, the resulting spin is below the Kerr limit ($q = 1$) and the final fate is likely to be a slowly rotating black hole. This result is due to the spin angular momentum being effectively transferred to orbital angular momentum via viscosity during the evolution.

For scenario (B), in which the corotation is not preserved for $\omega < \omega_{\text{vis}}$, we can consider two scenarios for the subsequent evolution. In one scenario, each star reaches a mass-shedding limit as a result of the decrease of stellar radius. It then evolves along a mass-shedding sequence ejecting mass from the equator until the onset of quasi-radial instability [7]. We refer to this scenario as scenario (Ba). As discussed in [7], the final fate of each star after the onset of the instability is not clear, since q is nearly equal to unity at the onset of the instability, and rotation may inhibit direct collapse to a black hole. In the other scenario, each star in the binary shrinks, conserving spin angular momentum through the entire evolution, until quasi-radial collapse. This is the case in which the stellar radius at $\omega = \omega_{\text{vis}}$ is sufficiently small to reach the turning points before reaching a mass-shedding limit. We refer to this scenario as scenario (Bb). In this case, q parameter could be smaller than unity so that the final outcome is likely to be a black hole of moderately large spin.

We derive the criterion for the stellar radius at $\omega = \omega_{\text{vis}}$ to follow scenario (Bb). From Eq. (2.21), the angular velocity of each star at $\omega = \omega_{\text{vis}}$ is

$$\Omega_0^2 \sim 7 \times 10^{-4} \alpha^{-1/2} \frac{M}{R_0^3} \left(\frac{M/R_0}{10^{-3}} \right)^{-5/4} \left(\frac{M}{10^6 M_\odot} \right)^{3/4}, \quad (5.9)$$

where R_0 is the stellar radius at $\omega = \omega_{\text{vis}}$. With decreasing stellar radius $R < R_0$, ω becomes smaller than ω_{vis} . For $\omega < \omega_{\text{vis}}$, the spin angular momentum of each star remains constant until the star reaches a mass-shedding limit at which the angular velocity approximately becomes [5–7]

$$\Omega_{\text{shed}}^2 \simeq \frac{8M}{27R^3}. \quad (5.10)$$

Because of the conservation of the spin angular momentum and mass, the relation, $R^2\Omega = R_0^2\Omega_0$, approximately holds. Hence,

$$\Omega^2 \sim 7 \times 10^{-4} \alpha^{-1/2} \frac{MR_0}{R^4} \left(\frac{M/R_0}{10^{-3}} \right)^{-5/4} \left(\frac{M}{10^6 M_\odot} \right)^{3/4}. \quad (5.11)$$

For the second scenario, Ω has to be less than Ω_{shed} at the onset of quasi-radial collapse, i.e.,

$$\frac{R}{R_0} \gtrsim 0.07 \alpha^{-2/9} \left(\frac{M/R}{10^{-3}} \right)^{-5/9} \left(\frac{M}{10^6 M_\odot} \right)^{1/3}. \quad (5.12)$$

Thus, R_0 has to be less than ~ 10 times of stellar radius at the onset of quasi-radial collapse for $M \sim 10^6 M_\odot$.

In Fig. 6, we present a schematic diagram for the evolution of supermassive binaries of $M = 10^6 M_\odot$ for $\alpha = 1$. The horizontal and vertical axes denote M/R and r/R , respectively. Since M is conserved and r remains approximately constant in negligible gravitational wave emission, evolution proceeds at fixed M/r approximately (see solid and dashed lines). A binary with $r/R < 2$ (below the lower long-dashed line) should be regarded as a single star, so that only the region with $r/R > 2$ is relevant here. Slowly rotating supermassive stars with $M/R \gtrsim 6.3 \times 10^{-4}$ and $S/M^2 \ll 1$ are unstable against quasi-radial collapse (the right-hand side of the vertical long-dashed line). A binary is corotating if it resides in the region surrounded by three long-dashed lines. A corotating binary with $r/R \gtrsim 4.1$ (above the dotted line) is secularly stable, so that if a corotating binary resides above (below) the dotted line, r/R increases (decreases) with evolution. (We note that for non-corotating binaries in which tidal, viscous effect is negligible, such secular instability would not exist, implying that r/R would always increase for them.)

From these results, we find the following conclusion for $M = 10^6 M_\odot$: (1) If M/R of a corotating binary is initially larger than $\sim 2 \times 10^{-4}$, the corotation is preserved until each supermassive star in the binary reaches the onset of quasi-radial collapse [scenario (A)]. In this case, the product is a binary black hole of small spin parameter. (2) If M/R of a corotating binary is initially larger than $\sim 6 \times 10^{-5}$, each supermassive star in the binary reaches the onset of quasi-radial collapse before reaching the mass-shedding limit [scenario (Bb)]. In this case, the product is a binary black hole of moderately large spin. (3) If M/R is initially smaller than $\sim 6 \times 10^{-5}$, stable, supermassive binary stars in corotation can never be achieved [scenario (Ba)]. In this case, the outcome is not clear. If the supermassive stars directly collapse to black holes conserving the spin and mass, the product would be a binary black hole of large spin $q \sim 1$.

VI. IMPLICATION FOR GRAVITATIONAL WAVE DETECTION

In this section, we estimate the frequency and amplitude of gravitational waves from supermassive binary stars in stable circular orbits and from collapse to a black hole [i.e. for scenario (A) and (Bb)]. Possibilities for generating burst and quasi-periodic gravitational waves after the onset of quasi-radial instability in scenario (Ba) are the same as those discussed in [7].

Frequency f and amplitude h of gravitational waves from supermassive binary stars in circular orbits are calculated as

$$f \sim 3 \times 10^{-6} \text{Hz} \left(\frac{1000M}{r} \right)^{3/2} \left(\frac{10^6 M_\odot}{M} \right), \quad (6.1)$$

$$h \sim 10^{-19} \left(\frac{1000M}{r} \right) \left(\frac{M}{10^6 M_\odot} \right) \left(\frac{3000 \text{Mpc}}{D} \right), \quad (6.2)$$

where D denotes the distance from the source to detectors. Since $r > 1000M$ for supermassive binary stars with $M > 4 \times 10^5 M_\odot$, the frequency is smaller than $\sim 3 \times 10^{-6}$ which is too low to be detected by LISA [2,3].

Close binaries will be secularly unstable to merger to a single rotating star. During merger, the coalesced object is likely to form a stable ellipsoid which could emit quasi-periodic gravitational waves. Even in this case, the frequency will be similar to that given in Eq. (6.1) and is still too low, since the radius of the ellipsoid is likely to be larger than $\sim 1000M$.

Supermassive stars in a stable binary orbit likely collapse to black holes after quasi-stationary contraction but prior to merger. For the case when the orbital separation and compactness of each star are initially small, the black holes

are directly formed after onset of quasi-radial instability according to scenarios (A) and (Bb). As we found in Sec. V, supermassive stars are rotating with $0.3 \lesssim q < 1$ at the onset of quasi-radial instability. Since the collapse is non-spherical, gravitational waves are emitted. Gravitational waves during formation of black holes are likely dominated by quasi-normal modes of black holes [24]. Perturbation studies for the frequency of quadrupole quasi-normal modes provide [25]

$$f \sim (0.03 - 0.08)M^{-1} \simeq (6 - 15) \times 10^{-3} \left(\frac{M}{10^6 M_\odot} \right)^{-1} \text{ Hz}, \quad \text{for } 0 \leq q < 1. \quad (6.3)$$

Thus, the frequency for $M \sim 10^6 M_\odot$ is in the range in which LISA is expected to be most sensitive. The strength of the gravitational wave signal likely depends strongly on q and on the dynamics of collapse, so that it is difficult to assess without numerical simulation. An order-estimate yields [11]

$$h \sim 10^{-19} \left(\frac{\varepsilon}{10^{-6}} \right)^{1/2} \left(\frac{10^{-3} \text{ Hz}}{f} \right)^{1/2} \left(\frac{3000 \text{ Mpc}}{D} \right) \left(\frac{M}{10^6 M_\odot} \right)^{1/2}, \quad (6.4)$$

where ε denotes the ratio of the total emitted energy of gravitational waves to the gravitational mass energy M . Thus, as long as $\varepsilon \gtrsim 10^{-10}$, detection of gravitational waves will be possible by LISA in which the sensitivity around $f \sim 10^{-3} \text{ Hz}$ is $\sim 10^{-21}$. A numerical relativistic work [24] indicates that ε depends strongly on q and initial conditions. Since the simulations in [24] are carried out only for collapse of neutron stars, it is necessary to perform a simulation preparing a realistic initial condition and using realistic soft equations of state for supermassive stars to clarify the magnitude of ε . However, Ref. [24] reports that as long as $q \gtrsim 0.2$, ε could be larger than 10^{-6} . If this relation would hold for collapse of supermassive stars, future detection of gravitational waves for scenarios (Ba) and (Bb) would be possible.

If supermassive stars eventually collapse to a black hole, a black hole binary will be formed and subsequently decreases orbital separation radiating gravitational waves during inspiraling in a timescale τ_{GW} [see Eq. (2.14)]. The frequency and amplitude are given by Eqs. (6.1) and (6.2), which show that supermassive binary black holes with $r \lesssim 200M(M/10^6 M_\odot)^{-3/2}$ emit gravitational waves of $f \gtrsim 10^{-4} \text{ Hz}$ and can be strong sources of LISA.

VII. SUMMARY

We have investigated equilibrium and stability of supermassive stars in two-body binary systems. We found that supermassive binary stars in close, corotating orbits with $r/R \lesssim 4(M/10^6 M_\odot)^{1/6}$ are secularly unstable. We also have shown that the corotation cannot be achieved for distant orbits with $r/R \gtrsim 12(M/10^6 M_\odot)^{-11/24}$, since the timescale for viscous transfer of the angular momentum is longer than the evolution timescale due to radiation of thermal energy. These facts suggest that existence of stable supermassive stars in corotating binaries is highly restricted. In particular for massive systems $M \gtrsim 6 \times 10^6 M_\odot$, corotation cannot be achieved. Evolution in such a massive binary does not experience transfer between orbital and spin angular momentum. Namely, the evolution of the velocity field of one star is not affected by its companion star. In this case, each supermassive star will be rapidly and rigidly rotating, as in the case of isolated supermassive stars.

As discussed in [7], rotating supermassive stars in isolation will evolve along a mass-shedding sequence to quasi-radial collapse. At the onset of the instability, the nondimensional spin parameter q is close to unity, suggesting that the collapsing star may not form a black hole in a straightforward manner. During the collapse, the centrifugal force may inhibit the collapse to a black hole near the equatorial plane to form a disk. After the formation of disk, non-axisymmetric instabilities may play an important role in forming a bar, or in fissioning to several blobs. On the other hand, if supermassive stars collapse directly to black holes, the resulting black holes will have a large spin near Kerr limit $q \sim 1$. Only numerical simulation in full general relativity can distinguish these fates.

For supermassive stars in binaries of fairly small mass $\lesssim 4 \times 10^6 M_\odot$, small initial orbital separation $r \sim 4R$, and initially small compactness, corotating orbits persist until the onset of quasi-radial collapse. In this case, the q parameter of each star at the onset of the instability is much less than unity since spin angular momentum can be transferred to orbital angular momentum by viscosity during the evolution. The final fate of the system is likely to be a binary black hole of small spin, although it is achieved for restricted initial conditions.

ACKNOWLEDGMENTS

We thank T. Baumgarte for helpful discussion and comments. M.S. thanks the Department of Physics of the University of Illinois at Urbana-Champaign (UIUC), where most of this work was done, for warm hospitality and

APPENDIX A: ROCHE BINARY

In this appendix, we briefly investigate equilibrium and stability of supermassive stars in the Roche binary. In this problem, we treat binaries composed of a point body of mass m and a supermassive star of mass M . We again assume that the equation of state for the supermassive star is given by Eq. (3.1). In this setting, the total energy of the system E is written in the form

$$E = k_1 K M x^{3/n} - k_2 M^{5/3} x - k_4 M^{7/3} x^2 - \frac{Mm}{r} + \frac{I}{2} \Omega^2 + \frac{Mm}{2(M+m)} r^2 \Omega^2, \quad (\text{A1})$$

where Ω here is determined by

$$\Omega = \sqrt{\frac{M+m}{r^3}}, \quad (\text{A2})$$

and other notations are the same as those in Sec. III. The total angular momentum is written

$$J = \frac{Mm}{M+m} r^2 \Omega + I \Omega = (\eta' \Omega^{-1/3} + \kappa x^{-2} \Omega) M^{5/3}, \quad (\text{A3})$$

where $\eta' \equiv m/(M+m)^{1/3} M^{2/3}$. Taking the first derivative of E with respect to x fixing M , J and K yields a condition for equilibrium

$$0 = \left. \frac{\partial E}{\partial x} \right|_{M,J,K} = \frac{3k_1}{n} K M x^{3\epsilon} - k_2 M^{5/3} - 2k_4 M^{7/3} x + \frac{\kappa \Omega^2 M^{5/3}}{x^3}, \quad (\text{A4})$$

where we use

$$\left. \frac{\partial \Omega}{\partial x} \right|_{M,J} = \frac{2\kappa}{x^3} \Omega \left(-\frac{\eta'}{3} \Omega^{-4/3} + \frac{\kappa}{x^2} \right)^{-1}. \quad (\text{A5})$$

Equation (A4) is completely the same as Eq. (3.13), implying that we can construct equilibria in the same manner as that in Sec. III.

The second derivative of E with respect to x becomes

$$\begin{aligned} \left. \frac{\partial^2 E}{\partial x^2} \right|_{M,J,K} &= \frac{9\epsilon k_1}{n} K M x^{3\epsilon-1} - 2k_4 M^{7/3} - \frac{3\kappa M^{5/3} \Omega^2}{x^4} \left(\frac{\eta' x^2 + \kappa \Omega^{4/3}}{\eta' x^2 - 3\kappa \Omega^{4/3}} \right) \\ &= 3\epsilon k_2 M^{5/3} x^{-1} - 2(1-3\epsilon)k_4 M^{7/3} - \frac{3\kappa \Omega^2 M^{5/3}}{x^4} \left(\frac{\eta' x^2 + \kappa \Omega^{4/3}}{\eta' x^2 - 3\kappa \Omega^{4/3}} + \epsilon \right). \end{aligned} \quad (\text{A6})$$

Thus, the stability can be investigated simply by exchanging η in Eq. (3.15) to η' , so that the qualitative feature on the stability is essentially the same as that shown in Sec. III. A sufficient condition for existence of a stable equilibrium in close orbits ($\partial^2 E / \partial x^2|_{M,J,K} > 0$) is given by

$$\epsilon k_2 - \kappa \omega^2 \left(\frac{\eta' + \kappa \omega^{4/3}}{\eta' - 3\kappa \omega^{4/3}} + \epsilon \right) > 0, \quad (\text{A7})$$

where

$$\omega^2 \equiv \frac{\Omega^2}{x^3} = \frac{4\pi}{3} \frac{\rho_m}{\rho_c} \left(1 + \frac{m}{M} \right) \left(\frac{R}{r} \right)^3. \quad (\text{A8})$$

Equation (A7) is approximately written as

$$\omega^2 < \frac{\epsilon k_2}{\kappa}. \quad (\text{A9})$$

Thus, we find that close orbits with $r \sim R$ are secularly unstable for a small value of ϵ , i.e., $\epsilon \lesssim 0.05(1 + m/M)$, in Roche binary.

In this section, we briefly review the effect of tidal energy to the equilibrium and stability of supermassive stars in binary systems. In the following, we consider supermassive binary stars of equal mass and of no spin for simplicity.

Including the tidal energy but neglecting the effect of the spin, the energy of one star is written as [19]

$$E = k_1 K M x^{3/n} - k_2 M^{5/3} x - k_4 M^{7/3} x^2 + \frac{M}{8} r^2 \Omega^2 - \frac{M^2}{2r} - \frac{\lambda M^{11/3}}{r^6 x^5}, \quad (\text{B1})$$

where Ω is determined from $\partial E / \partial r|_{M,J,K} = 0$ as

$$\Omega = \sqrt{\frac{2M}{r^3} + \frac{24\lambda M^{8/3}}{r^8 x^5}}, \quad (\text{B2})$$

and

$$\lambda = \frac{75}{16} \kappa^2 \left(1 - \frac{n}{5}\right) \left(\frac{3\rho_c}{4\pi\rho_m}\right)^{1/3}. \quad (\text{B3})$$

Our notation is the same as that in Sec. III, except that the angular momentum of one star is written as

$$J = \frac{Mr^2}{4} \Omega. \quad (\text{B4})$$

Taking the first derivative of E with respect to x fixing M , J and K yields a condition for equilibrium

$$0 = \frac{\partial E}{\partial x} \Big|_{M,J,K} = \frac{3k_1}{n} K M x^{3\epsilon} - k_2 M^{5/3} - 2k_4 M^{7/3} x + \frac{5\lambda M^{5/3}}{64} \left(\frac{3\rho_c}{4\pi\rho_m}\right)^{-2} \left(\frac{2R}{r}\right)^6, \quad (\text{B5})$$

where we use

$$\frac{\partial r}{\partial x} \Big|_{M,J} = \frac{60\lambda M^{5/3}}{r^4 x^6} \left(1 - \frac{48\lambda M^{5/3}}{x^5 r^5}\right)^{-1}. \quad (\text{B6})$$

For $n = 3$, $\lambda \simeq 0.76$, and the fourth term of Eq. (B5) is written for $n = 3$ as $3.5 \times 10^{-4} M^{5/3} (2R/r)^6$. Comparing with Eq. (3.13), it is found that the magnitude of the tidal energy is by a factor $\sim 0.02(2R/r)^3$ smaller than the magnitude of the spin effect for corotating binaries, implying that the effect of the tidal energy for equilibria of supermassive stars is much less important.

The second derivative of E with respect to x becomes

$$\begin{aligned} \frac{\partial^2 E}{\partial x^2} \Big|_{M,J,K} &= \frac{9\epsilon k_1}{n} K M x^{3\epsilon-1} - 2k_4 M^{7/3} - \frac{30\lambda M^{11/3}}{r^6 x^7} \frac{x^5 r^5 + 12\lambda M^{5/3}}{x^5 r^5 - 48\lambda M^{5/3}} \\ &= 3\epsilon k_2 M^{5/3} x^{-1} - 2(1 - 3\epsilon) k_4 M^{7/3} - \frac{15\lambda M^{5/3}}{32x} \left(\frac{2R}{r}\right)^6 \left(\frac{3\rho_c}{4\pi\rho_m}\right)^{-2} \left(\frac{x^5 r^5 + 12\lambda M^{5/3}}{x^5 r^5 - 48\lambda M^{5/3}} + \frac{\epsilon}{2}\right). \end{aligned} \quad (\text{B7})$$

Thus, the condition for existence of stable supermassive stars is approximately written as

$$\epsilon > \frac{5\lambda}{32} \left(\frac{3\rho_c}{4\pi\rho_m}\right)^{-2} \left(\frac{2R}{r}\right)^6 \sim 7 \times 10^{-4} \left(\frac{2R}{r}\right)^6. \quad (\text{B8})$$

In determining the stability of the non-spinning binary system, the tidal energy can be important for very small ϵ as $\epsilon < 10^{-3}$ and for very close orbits with $r \sim 2R$. However, as long as $\epsilon \gtrsim 7 \times 10^{-4}$, it is not important at all.

[1] M. J. Rees, in *Black holes and relativistic stars*, ed. R. M. Wald (Chicago University Press, 1998), 79.

- [2] For example, K. S. Thorne, in *Proceeding of Snowmass 95 Summer Study on Particle and Nuclear Astrophysics and Cosmology*, eds. E. W. Kolb and R. Peccei (World Scientific, Singapore, 1995), p. 398, and references therein.
- [3] P. Bender et al., LISA Pre-Phase A Report, Second Edition, MPQ 223, July, 1998
- [4] M. C. Begelman and M. J. Rees, Mon. Not. R. Astr. Soc. **185**, 847 (1978); M. J. Rees, ARA & A, **22**, 471 (1984); S. L. Shapiro and S. A. Teukolsky, Astrophys. J. Lett. **292**, L91 (1985); G. D. Quinlan and S. L. Shapiro, Astrophys. J. **356**, 483 (1990).
- [5] Ya. B. Zeldovich and I. D. Novikov, Relativistic Astrophysics, Vol. 1 (University of Chicago Press, 1971).
- [6] S. L. Shapiro and S. A. Teukolsky, *Black Holes, White Dwarfs, and Neutron Stars* (Wiley Interscience, New York, 1983), chapter 17.
- [7] T. W. Baumgarte and S. L. Shapiro, Astrophys. J. **526**, 941 (1999).
- [8] A. Loeb and F. A. Rasio, Astrophys. J. **432**, 52 (1994).
- [9] e.g., H. Komatsu, Y. Eriguchi and I. Hachisu, Mon. Not. R. astr. Soc. **237**, 355 (1989); G. B. Cook, S. L. Shapiro and S. A. Teukolsky, Astrophys. J. **398**, 203 (1992); S. Bonazzola, E. Gourgoulhon, M. Salgado and J.-A. Marck, Astron. Astrophys. **278**, 421 (1993).
- [10] But, see the following reference for an alternative scenario where supermassive stars are assumed to maintain differential rotation: K. C. B. New and S. L. Shapiro, Astrophys. J. in press (2000); astro-ph/0010172.
- [11] K. S. Thorne, in *300 years of gravitation*, eds. S. W. Hawking and W. Israel (Cambridge University Press, 1987), 330.
- [12] e.g., C. Cutler and E. E. Flanagan, Phys. Rev. D **49**, 2658 (1994).
- [13] S. Chandrasekhar, Astrophys. J. **140**, 417 (1964).
- [14] K. J. Fricke, Astrophys. J. **183**, 941 (1973); G. M. Fuller, S. E. Woosley and T. A. Weaver, Astrophys. J. **307**, 675 (1986).
- [15] e.g., Ref. [6], chapter 16.
- [16] J.-L. Tassoul, *Stellar Rotation* (Cambridge University Press, 2000).
- [17] N. I. Shakura and R. A. Sunyaev, Astron. and Astrophys. **24**, 337 (1973).
- [18] D. Lai, F. A. Rasio, and S. L. Shapiro, Astrophys. J. suppl. **88**, 205 (1993).
- [19] D. Lai, Phys. Rev. Lett. **76**, 4878 (1996).
- [20] R. Sorkin, Astrophys. J. **249**, 254 (1981); J. R. Ipser and G. Horowitz, Astrophys. J. **232**, 863 (1979); J. Katz, Mon. Not. R. astr. Soc. **183**, 765 (1978); J. L. Friedman, J. R. Ipser and R. D. Sorkin, Astrophys. J. **325**, 722 (1988); T. W. Baumgarte, G. B. Cook, M. A. Scheel, S. L. Shapiro, and S. A. Teukolsky, Phys. Rev. D **57**, 6181 (1998).
- [21] T. W. Baumgarte, G. B. Cook, M. A. Scheel, S. L. Shapiro, and S. A. Teukolsky, Phys. Rev. D **57**, 7299 (1998).
- [22] M. Shibata, Phys. Rev. D **60**, 104052 (1999).
- [23] K. Uryū and Y. Eriguchi, Phys. Rev. D **61**, 124023 (2000).
- [24] R. F. Stark and T. Piran, Phys. Rev. Lett. **55**, 891 (1985); T. Piran and R. F. Stark, in *Dynamical Spacetimes and Numerical Relativity*, ed. J. M. Centrella (Cambridge University Press, 1986), 40.
- [25] E. W. Leaver, Proc. R. Soc. London **A402**, 285 (1985).

TABLE I. Nondimensional structure constant for Newtonian spherical polytrope with $n \simeq 3$. ϵ denotes $1/n - 1/3$.

ϵ	ξ_1	$ \theta(\xi_1) $	k_1	k_2	k_4	κ	ρ_c/ρ_m	C_c	q_0
0	6.89685	0.0424298	1.75579	0.639000	0.918294	0.415248	54.1825	0.44465	0.4065
0.0001	6.89334	0.0424785	1.75520	0.639006	0.918215	0.415118	54.0928	0.44512	0.4062
0.001	6.86202	0.0429176	1.74992	0.639654	0.917504	0.413954	53.2960	0.44929	0.4042
0.003	6.79394	0.0438962	1.73829	0.640950	0.915917	0.411410	51.5909	0.45866	0.3997
0.005	6.72789	0.0448786	1.72679	0.642233	0.914321	0.408923	49.9711	0.46814	0.3954

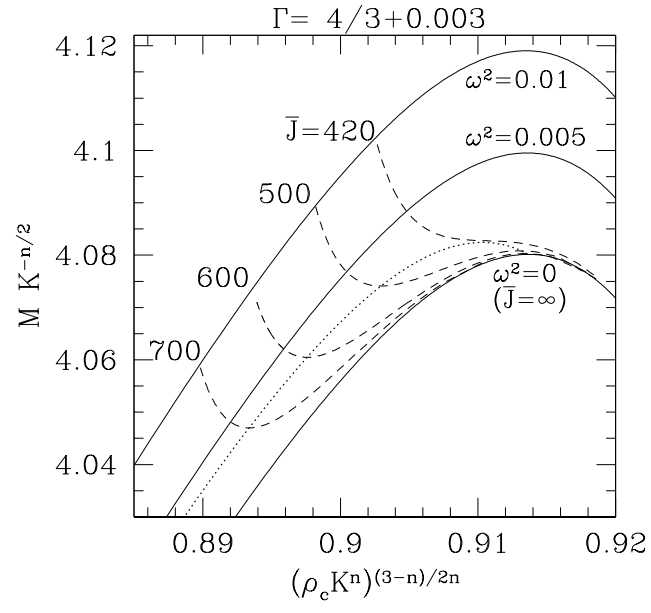
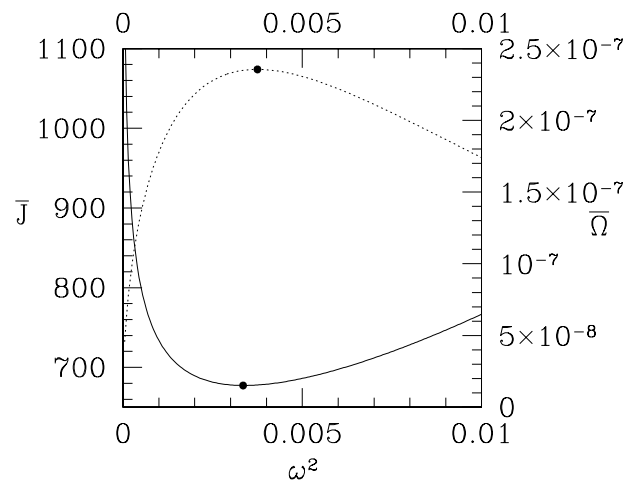
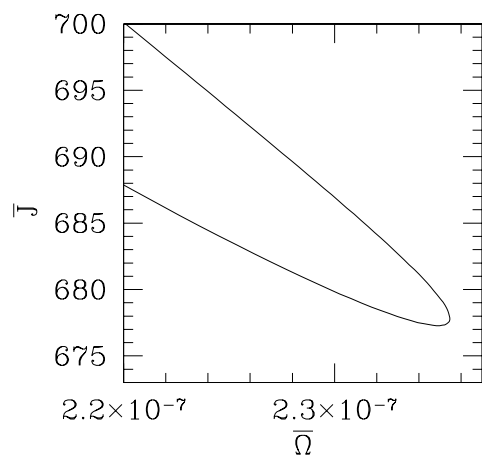


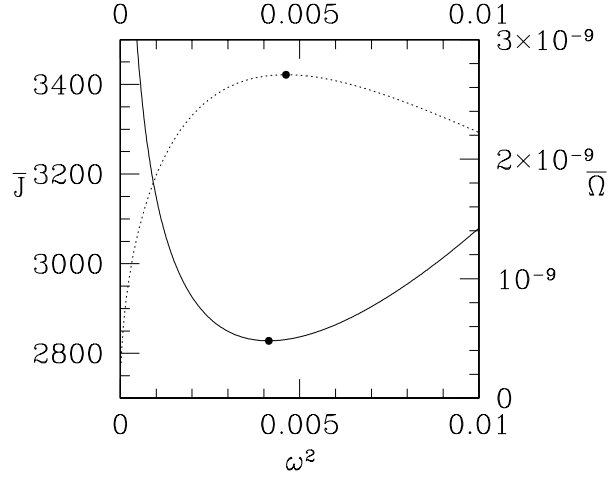
FIG. 1. Analytic mass-density relation for $\epsilon = 0.003$. The dependence of \bar{M} on $\bar{\rho}_c^{(3-n)/2n}$ for fixed values of ω^2 is indicated by the solid lines. The dependence of \bar{M} on $\bar{\rho}_c^{(3-n)/2n}$ for fixed values of \bar{J} is shown by the dashed lines. The dotted line indicates the sequence of the turning points.



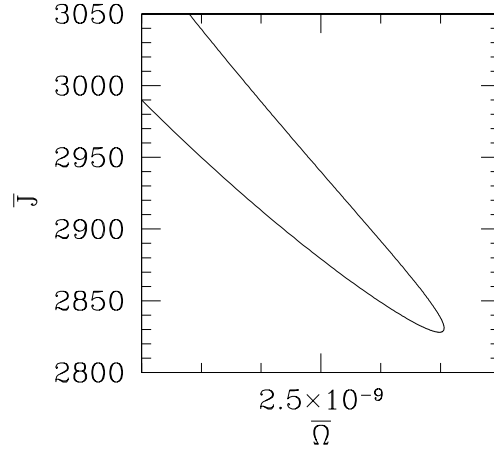
(a)



(b)



(c)



(d)

FIG. 2. (a) \bar{J} (solid curve) and $\bar{\Omega}$ (dotted curve) as a function of ω^2 along a fixed value of \bar{M} ($= 4.05$) for $\epsilon = 0.003$. Two solid circles indicate the minimum of \bar{J} and maximum of $\bar{\Omega}$. (b) Relation between \bar{J} and $\bar{\Omega}$ near the minimum of \bar{J} for $\bar{M} = 4.05$ and $\epsilon = 0.003$. (c) The same as (a) but for $\bar{M} = 3.90$. (d) The same as (b) but for $\bar{M} = 3.90$.

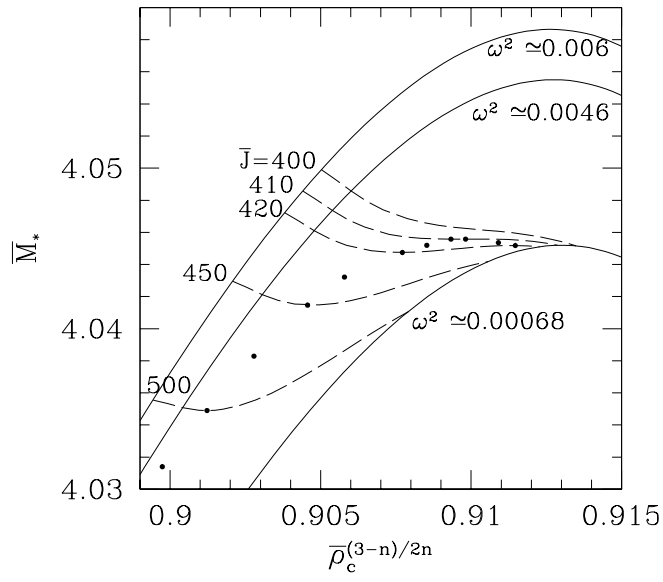


FIG. 3. Numerical mass-density relation for $\epsilon = 0.003$. The dependence of \bar{M} on $\bar{\rho}_c^{(3-n)/2n}$ for fixed values of ω^2 is indicated by the solid lines. The dependence of \bar{M} on $\bar{\rho}_c^{(3-n)/2n}$ for fixed values of \bar{J} is shown by the dashed lines. The solid dots indicate the sequence of the turning points.

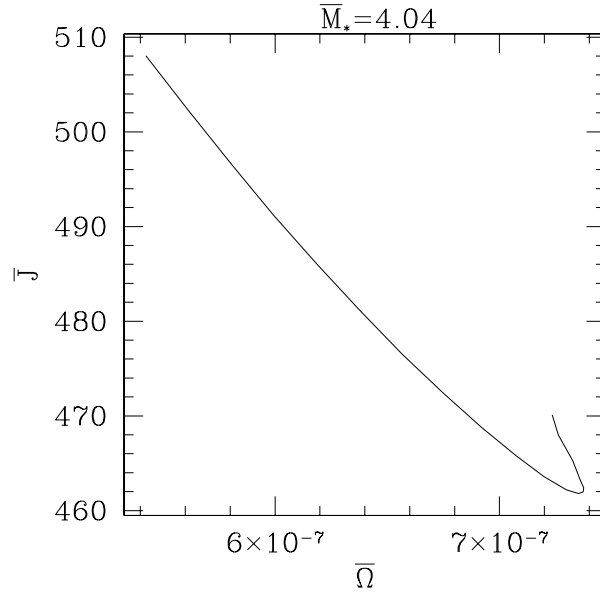


FIG. 4. Numerical relation between \bar{J} (solid curve) and $\bar{\Omega}$ for a given value of \bar{M}_* ($= 4.04$) for $\epsilon = 0.003$.

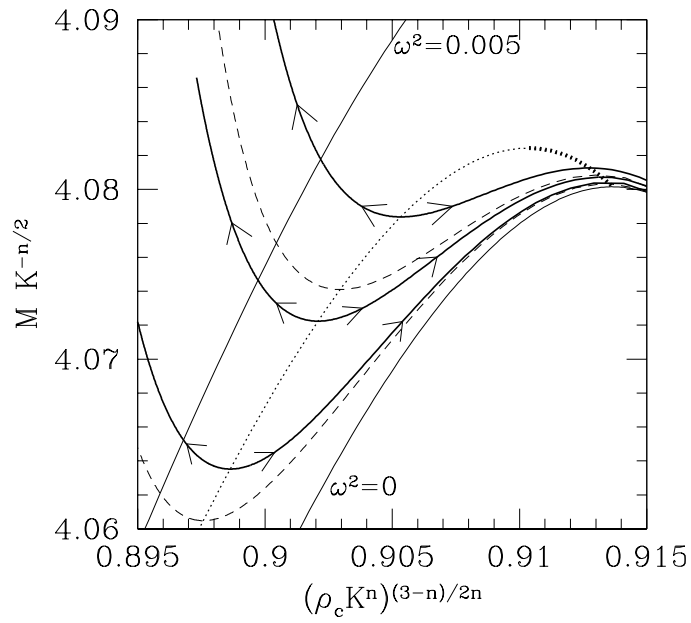


FIG. 5. Evolutionary tracks along curves of fixed \bar{J}/\bar{M}^2 ($= 28, 31$ and 35 , thick solid lines from top to bottom) for $\epsilon = 0.003$. The evolution must proceed toward increasing \bar{M} as indicated by arrows. The thin solid lines denote fixed values of ω and the dashed lines show curves of fixed value of \bar{J} ($= 500$ (upper) and 600 (lower)), used to determine the location of turning points (dotted line). The thin dotted line marks the threshold between increasing and decreasing orbital separation. The thick dotted line marks the onset of quasi-radial collapse.

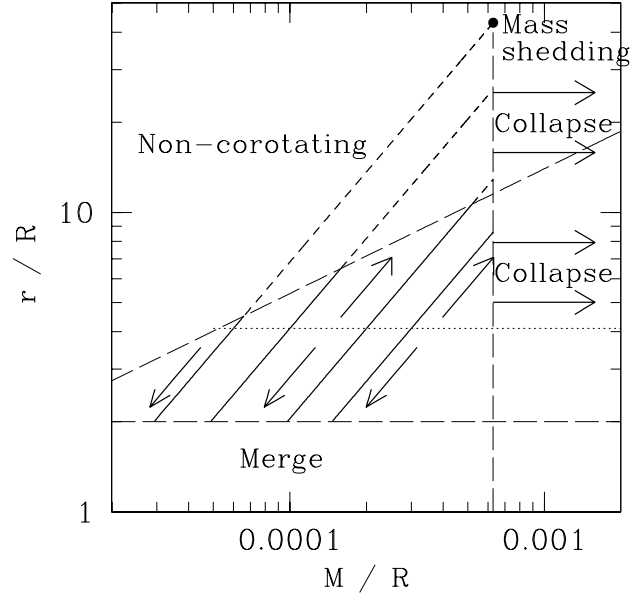


FIG. 6. Schematic diagram for the quasi-stationary evolution of supermassive binary stars of equal mass. The solid arrows indicate the direction of evolution as a result of cooling via thermal radiation. The solid and dashed lines indicate possible evolutionary paths.